Thin Solid Films 544 (2013) 537–540

Contents lists available at ScienceDirect

Thin Solid Films

journal homepage: www.elsevier.com/locate/tsf

Impact of plasma treatment on structure and electrical properties of porous low dielectric constant SiCOH material

Yi-Lung Cheng [a,*], Jun-Fu Huang [a], Yu-Min Chang [b], Jihperng Leu [b]

[a] Department of Electrical Engineering, National Chi-Nan University, Nan-Tou, Taiwan, ROC
[b] Department of Material Science and Engineering, National Chiao-Tung University, Shin-Chu, Taiwan, ROC

ARTICLE INFO

Available online 31 December 2012

Keywords:
Low-*k* dielectric
H_2/He
Plasma
Remote plasma
Reliability
Breakdown

ABSTRACT

Low dielectric constant (low-*k*) porous films are needed for advanced technologies to improve signal propagation. The integration of porous low-*k* films faces more severe challenges due to the presence of porosity. Plasma treatments have been considered to be critical steps to impact the low-*k* films' properties. In this study, the effect of various H_2/He plasma treatments on the porous low-*k* dielectrics deposited by plasma enhanced chemical vapor deposition was investigated. All the plasma treatments resulted in the formation of a thin and dense layer on the surface of the porous low-*k* films. Additionally, the properties of this top dense layer are modified and changed for the standard H_2/He plasma treatment, leading to a degraded electrical and reliability performance. However, H_2/He plasma-treated low-*k* dielectric by the remote plasma method shows a better electrical and reliability performance. As a result, the remote plasma treatment on the porous low-*k* dielectrics appears to be a promising method in the future interlayer dielectrics application.

1. Introduction

As feature sizes of integrated circuits continuously shrink to sub-micro, interconnect resistance-capacitance (RC) delay begins to dominate overall device speed in copper (Cu)/low dielectric (low-*k*) metallization. To decrease RC delay time, interconnection resistance has been reduced using Cu instead of aluminum while interlayer capacitance has been lowered by replacing conventional silicon dioxide (k~4.0) with low-*k* materials (k<4.0) [1–3].

For low-*k* materials, they should introduce the porosity within the film in order to reduce the permittivity below 2.5 [4,5]. However, the porous low-*k* materials would suffer multiple challenges to their integration in the damascene interconnects either due to their mechanical weakness or the degradation during integration [6]. Additionally, in the integration process, the plasma treatments are indispensible step, and are thought to be one of the most critical steps in regarding to the modification of the porous material [7,8].

Before Cu barrier layer was deposited, H_2/He plasma treatment was commonly used to reduce CuO_x layer [9,10]. At the same time, this plasma treatment was also performed on the neighboring low-*k* materials. Understanding of the plasma damage mechanism on the low-*k* materials is therefore one of the key factors for interconnect integration. This work investigates the impact of the various H_2/He plasma treatments on the physical, electrical properties, and reliability of the porous low-*k* film. The dielectric reliabilities and the integrated interline electromigration (EM) are also examined.

2. Experimental details

The as-deposited porous low-*k* material is a SiCOH film, deposited on a p-type (100) silicon substrates by plasma enhanced chemical vapor deposition (PECVD). The porous low-*k* films were deposited from diethoxymethylsilane and alpha-terpiene as a matrix and porogen precursor, respectively. A small amount of oxygen was also introduced as an oxidant. The deposition temperature, pressure, and power were 300 °C, 1.0×10^4 Pa, and 600 W, respectively. After deposition, UV curing with 200–450 nm wavelength was performed to remove the organic porogen. The average pore size and porosity of the resulting porous low-*k* films are around 1.4 nm and 12%, respectively, which were determined from the isotherm of ethanol adsorption and desorption using ellipsometric porosimetry. The dielectric constant is ~2.54. Then, the porous low-*k* film (blanket wafer) was tested by various H_2/He plasma treatments, whose conditions are listed in Table 1.

The thickness and refractive index (at a 633 nm wavelength) of as-deposited films were analyzed on an optical-probe system with an ellipsometer. The water contact angle (WCA) was determined as the average of five measurements (Reme Hardt, Mode 100-00-230). The chemical composition of low-*k* films was identified using atomic compositional depth profile analysis (AES) with 5 keV Ar ion sputtering (VG Scientific Microlab 350). The electrical characteristics of low-*k* films were examined by capacitance–voltage measurements at 1 MHz using a semiconductor parameter analyzer (HP4280A). Leakage and breakdown measurements were done at room temperature (25 °C) on metal–insulator–silicon (MIS) and 0.126 μm-pitched line-to-line comb structures. The breakdown voltage is defined as the voltage at a sudden rise of at least three decades of the leakage current. The MIS

---

* Corresponding author. Tel.: +886 49 2910960 4987; fax: +886 49 2917810.
E-mail address: yjcheng@ncnu.edu.tw (Y.-L. Cheng).

0040-6090/$ – see front matter © 2012 Elsevier B.V. All rights reserved.
http://dx.doi.org/10.1016/j.tsf.2012.12.074

Table 1
Plasma treatment conditions performed on porous low-*k* material.

Plasma treatment	Reactor condition	Gas ratio	Component	Integration goal
Standard H_2/He treatment (STD)	Capacitive coupling plasma 750 W/room temperature	5% H_2/95% He	Deep UV, ion radical H_2/He	Chemical reduction of CuO_x
Remote H_2/He treatment	Two chambers: (1) Plasma generator chamber: Inductive coupling plasma 4000 W/room temperature (2) Reaction chamber: 0 W/300 °C	5% H_2/95% He	Radical H_2/He	Chemical reduction of CuO_x

capacitors with *p*-type silicon as the substrates and aluminum as the metal electrodes were fabricated. The thickness of low-*k* dielectric is 0.3 μm. The capacitors had an area of 30 × 30 μm^2. The line-to-line comb structure of 0.126 μm pitch and 0.062 μm Cu line width was fabricated using Cu single damascene process. EM test structure of 250 μm length and 0.062 μm width was fabricated using Cu double-layered dual damascene interconnect. After etching the low-*k* dielectric layer, various H_2/He plasma treatments were performed before Cu interconnects deposition. A 30 nm dielectric barrier of SiCN was deposited on the top of Cu lines using PECVD after completing Cu chemical mechanical polishing process. The stress temperature was 275 °C at a fixed current density of 2.0 MA/cm^2 for EM test. A sample size of 30 samples was used for each experiment. Resistance increase with time was monitored until failure. A failure criterion of 10% resistance increase was employed. More details on test structure fabrication and EM characterization can be found elsewhere [11].

3. Results and discussion

Fig. 1 shows the thickness variations of porous low-*k* films after the various H_2/He plasma treatments. We used a bi-layer model of ellipsometry measurement to measure the thickness and refractive index of the top modification layer and the bottom bulk low-*k* film. As shown, a thin modification layer was formed on the top of the porous low-*k* films after the plasma treatment. Additionally, the thickness of the top modification layer is dependent on the plasma treatment time and method. The thickness of the modified top layer increased with increasing the plasma treatment time. Moreover, in comparison to the standard plasma treatment, the remote plasma treatment can lead to a thinner thickness of the modified top layer. Furthermore, the thickness shrinkage in the bulk low-*k* film after the plasma treatment was also observed. The thickness shrinkage is obvious for the standard plasma treatment and becomes larger with increasing the treatment time. The results of refractive index also follow this trend. For the remote plasma treated sample, the refractive indexes of the modified top layer and the refractive index of the bulk low-*k* film remained unchanged with a value of 1.451. As for the standard H_2/He plasma treated samples, the refractive indexes of the modified top layer and bulk low-*k* film increased to 1.497 and 1.467, respectively. The results indicate that in addition to ion bombardment effect, the deep UV light emitted by the H_2/He plasma in the standard plasma condition reduces the bulk low-*k* film thickness and modifies the top thin layer. On the other hand, there are only radicals without deep UV light and ion bombardment in the remote H_2/He plasma condition. The radicals only modify the top thin layer and this effect is relatively weak.

To further investigate the properties of the modified top layer and the bulk low-*k* film, we used the diluted HF solution (1% volume) to etch the plasma-treated low-*k* materials with different times. The results of the etching rates for the modified top layer and the bulk low-*k* film are shown in Fig. 2. For plasma-treated low-*k* films using the remote H_2/He plasma, the etching rates of the modified top layer and the bulk low-*k* film are comparable, which have a similar value to that of non-treated samples. This indicates that the top modification layer induced by the remote H_2/He plasma treatment has a similar film property as the bulk low-*k* film. In the case of the standard H_2/He plasma-treated low-*k* films, the etching rates of the modified top layer are increased to ~50 and ~67 nm/min for 25 s and 100 s treated samples, respectively. Moreover, the etching rates of the bulk low-*k* film are also increased to ~17 nm/min. The results indicate that the properties of the top layer and the bulk low-*k* film treated by the standard H_2/He plasma are modified, which are different from those induced by the remote plasma treatment or the pristine low-*k* film. It can be further deduced that the top modification layer induced by deep UV light, ion bombardment, and radicals in the standard plasma condition is totally changed and have distinct film properties. However, this layer induced only by radicals in the remote plasma condition remains the similar characteristics as the pristine low-*k* film.

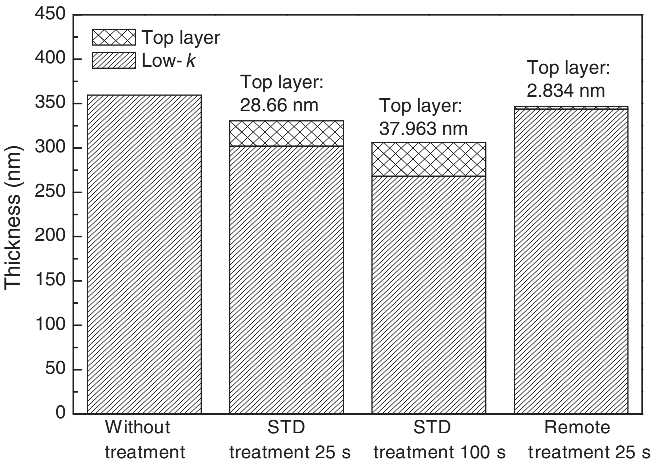

Fig. 1. Thickness variation of low-*k* films after the different plasma treatments.

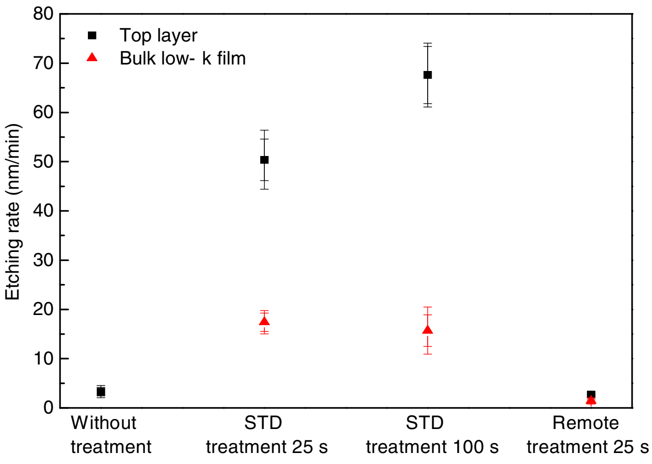

Fig. 2. Comparison on wet etching rate of various plasma-treated low-*k* films.

Further investigation the top modification layer was performed using AES analysis. Fig. 3 shows the depth profile of the carbon content in the plasma treated film, indicating that the carbon content decreases in the top modification layers induced by the standard H_2/He plasma treatment. Moreover, the depth of the damage layer (carbon loss) is lager for the standard H_2/He plasma treatment and becomes larger with increasing the treatment time. In the case of the remote H_2/He plasma-treated sample, the carbon profile remained unchanged, which is consistent with the result of Fourier transform infrared spectroscopy (Nicolet 460).

WCA measurements were performed to check the low-*k* films' hydrophilization after the various H_2/He treatments. The averaged results from 5 sites are shown in Fig. 4. A larger WCA (~90°) was observed for the porous low-*k* film without plasma treatment, indicating this porous low-*k* film seems to be hydrophobic. As expected, the WCA value of the remote H_2/He plasma-treated low-*k* films is not degraded, instead of slightly increase possibly due to moisture desorption, indicating that the porous low-*k* film after the remote plasma treatment becomes more hydrophobic. On the other hand, the WCA value is decreased for the standard plasma-treated low-*k* films, and the magnitude is amplified with enlarging the treatment time. This result indicates that the porous low-*k* films treated by the standard H_2/He plasma attack have lost their hydrophobic property and become hydrophilic, leading to a water-uptake.

Dielectric constants of the porous low-*k* films after the various H_2/He plasma treatments are shown in Fig. 5. The dielectric constant of as deposited porous low-*k* films after UV curing process is 2.54. After performing the remote plasma treatment, the dielectric constant of the porous low-*k* films decrease to 2.48. On the other hand, the dielectric constants increase and become larger with increasing the treatment time for the standard plasma treatment. This implies that the dielectric property of the porous low-*k* film layer treated by the standard H_2/He plasma was deteriorated.

The leakage currents of the porous low-*k* films after various H_2/He treatments were evaluated. Two tested structures: MIS and line-to-line comb structures (pitch/line = 0.126 μm/0.062 μm), were used to measure the dielectric property of the low-*k* films under various H_2/He treatments. Fig. 6 compares the leakage currents at 2 MV/cm for the porous low-*k* films after various H_2/He plasma treatments in two different structures. As shown, the leakage currents remain unchanged for both H_2/He plasma treatment methods in the MIS structure. For the standard H_2/He treatment with 100 s treatment time, the leakage current slightly increases by only ~2%. However, in the case of the line-to-line comb structures, the leakage current is related to the plasma treatment method and plasma treatment time. The remote plasma treated sample shows the comparable line-to-line leakage current as that without plasma treatment, but shows a better line-to-line leakage current than that of the standard plasma treated sample. Moreover, for the standard plasma treated sample, line-to-line leakage current becomes worse with increasing the plasma treatment time. This also demonstrates that the standard plasma treatment deteriorates the dielectric property of the porous low-*k* films. Moreover, a different behavior in the leakage current for these two structures was observed, indicating that the top modification layer induced by H_2/He plasma treatment has different effects on the leakage current of the porous low-*k* films. For MIS structures, this top modification layer has no significant impact on the leakage current due to a relatively thinner thickness in comparison to the bulk low-*k* film. On the contrary, in the line-to-line comb structures, this modified top layer between two conductors plays an important role in the leakage current. The modified top layer induced by the deep UV light and ion bombardment in the standard H_2/He plasma treatment becomes an activating diffusion path, increasing the leakage current. Based on the results, we can also infer that the leakage conduction mechanism between the conductors is dominated by the surface migration, rather than by the bulk film diffusion for the line-to-line comb structures.

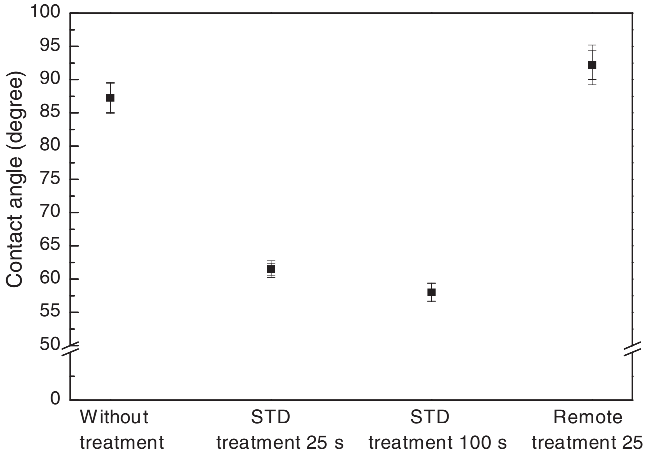

Fig. 4. Water contact angle of low-*k* films after various plasma treatments.

To further understand the dielectric reliability, voltage ramping-up to dielectric breakdown of the porous low-*k* under various plasma treatment conditions was measured. Fig. 7 shows the distributions of voltage ramping-up to dielectric breakdown of the porous low-*k*

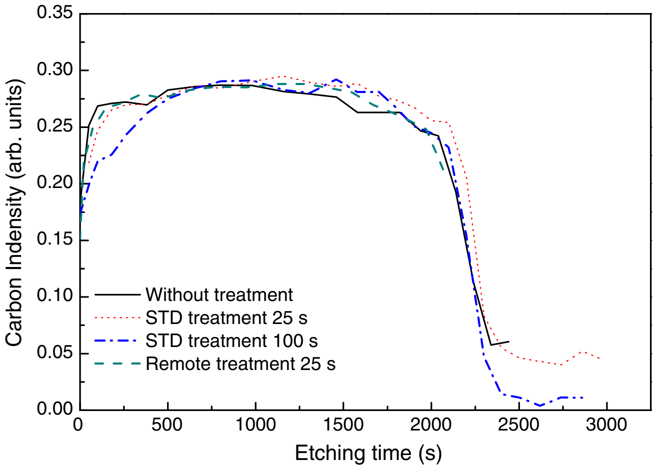

Fig. 3. Carbon AES profile of low-*k* films after various plasma treatments.

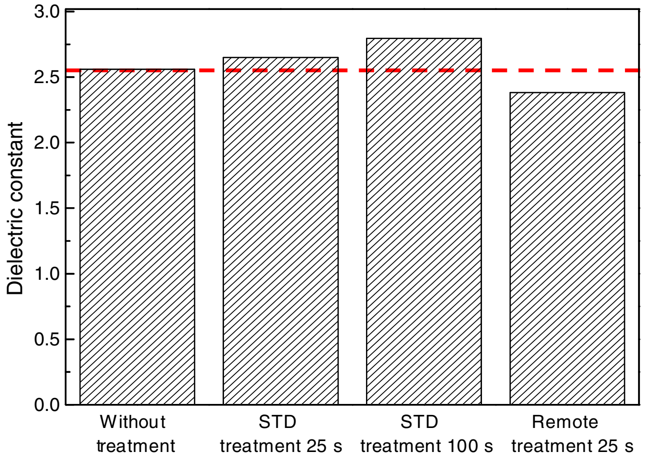

Fig. 5. Dielectric constants of low-*k* films after the different plasma treatments.

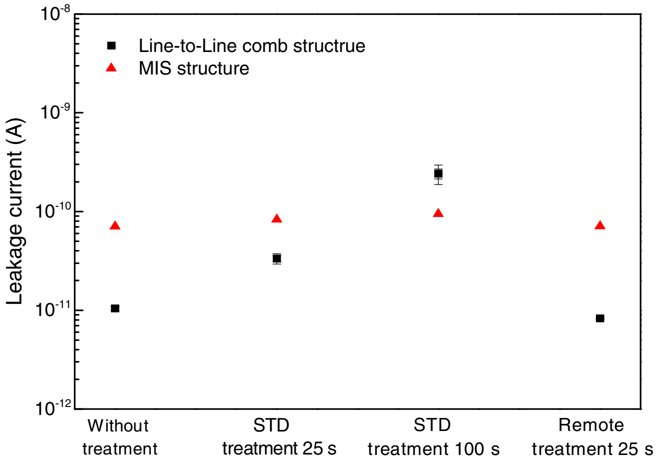

Fig. 6. Leakage current density at 2 MV/cm of low-*k* films after various plasma treatments in different test structures.

under various plasma treatments using line-to-line comb structures. As shown, the remote plasma treated sample has better voltage ramping-up to dielectric breakdown performance, while the standard plasma treated sample shows a lower breakdown voltage as compared to the non-treated sample. Moreover, the dielectric breakdown voltage becomes lower as the plasma treatment time increases. This also demonstrates that the standard plasma treatment with deep UV light radiation and ion bombardment degrades the low-*k* film reliability.

Fig. 8 presents the cumulative failure distribution of EM lifetime for typical Cu interconnect lines. The cumulative failure distribution is plotted by measurement of 30 sample's failure times using lognormal distribution. Although the difference of the measured failure times of Cu interconnect lines is not significantly large, it also can be observed that the failure times of Cu interconnect lines with the standard H_2/He treatment slightly decrease and become worse with increasing the treatment time. More obviously, the failure times of early failure samples degrade significantly for the standard H_2/He treatment condition with a longer treatment time. It is well known that the EM performance is controlled by the Cu interface and the bulk Cu film [12]. Therefore, the worse integrity between the plasma-treated low-*k* film and the Cu line at the side walls leads to a decreasing EM failure time for the standard plasma treatment condition.

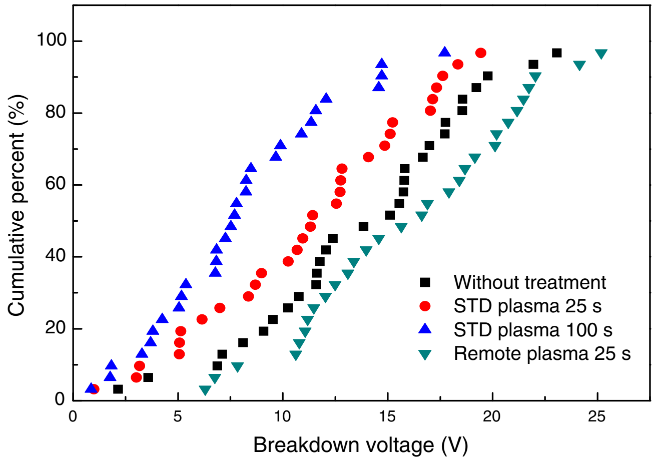

Fig. 7. Distribution of voltage ramping-up to dielectric breakdown for low-*k* films with different plasma treatments.

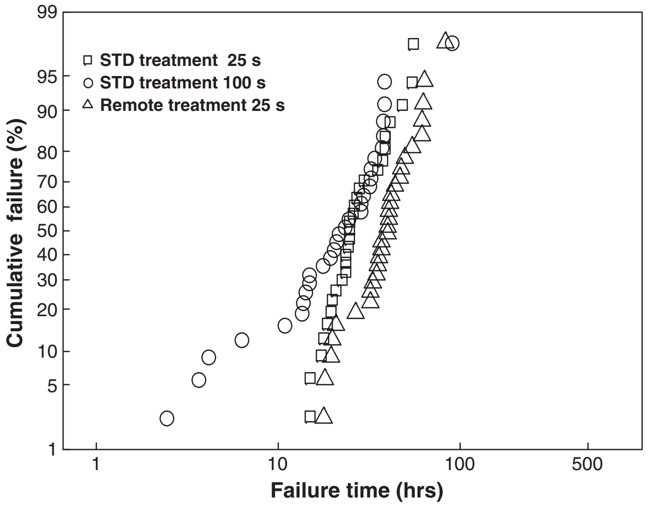

Fig. 8. EM lifetime cumulative failure distribution of Cu interconnect lines for low-*k* films with different plasma treatments.

4. Conclusions

In this study, the effect of various plasma treatments on the porous low-*k* dielectrics deposited by PECVD was investigated. All the plasma treatments resulted in the formation of a thin and dense layer on the surface of the porous low-*k* films. Additionally, the properties of this top dense layer are modified and changed for the standard H_2/He plasma treatment, causing the degraded electrical and reliability performance. However, H_2/He plasma-treated low-*k* dielectric by the remote plasma method shows a better electrical and reliability performance. As a result, the remote plasma treatment on the porous low-*k* dielectrics without deep UV light and ion bombardment appears to be a promising method in the future interlayer dielectrics application.

Acknowledgment

The author would like to thank the National Science Council of the Republic of China, Taiwan, for financially supporting this research under contract no. NSC-99-2221-E-260-002. Ted Kony is appreciated for his editorial assistance.

References

[1] A. Grill, J. Appl. Phys. 93 (2003) 1786.
[2] S.M. Gates, D.A. Neumayer, M.H. Sherwood, A. Grill, X. Wang, M. Sankarapandian, J. Appl. Phys. 101 (2007) 094103.
[3] C.Y. Kim, R. Navamathavan, H.S. Lee, J.K. Woo, M.T. Hyun, K.M. Lee, W.Y. Jeung, C.K. Choi, Thin solid Films 519 (2011) 5732.
[4] L. Broussous, G. Berthout, D. Rebiscoul, V. Rouessac, A. Ayral, Microelectron. Eng. 87 (2010) 466.
[5] C.H. Huang, N.F. Wang, Y.Z. Tsai, C.I. Hung, M.P. Houng, Microelectron. Eng. 87 (2010) 1735.
[6] H.G. Peng, D.Z. Chi, W.D. Wang, J.H. Li, K.Y. Zeng, R.S. Vallery, W.E. Frieze, M.A. Shalsey, D.W. Gidley, A.F. Yee, J. Electrochem. Soc. 154 (2007) G85.
[7] H.W. Guo, L. Zhu, L. Zhang, S.J. Ding, D.W. Zhang, R. Liu, Microelectron. Eng. 85 (2008) 2114.
[8] W. Puyrenier, V. Rouessac, L. Broussous, D. Rebiscoul, A. Ayral, Microelectron. Eng. 83 (2006) 2314.
[9] P. Verdonck, M. Aresti, A. Ferchichi, E.V. Besien, B. Stafford, C. Trompoukis, D.D. Roest, M. Baklanov, Microelectron. Eng. 88 (2011) 627.
[10] N. Posseme, T. Chevolleau, T. David, J. Vac. Sci. Technol. B 25 (2007) 1928.
[11] Y.L. Cheng, W.Y. Chang, Y.L. Wang, J. Vac. Sci. Technol. B 28 (2010) 573.
[12] A.V. Vairagar, S.G. Mhaisalkar, A. Krishnamoorthy, Thin Solid Films 462 (2004) 325.